Reports of Practical Oncology and Radiotherapy 25 (2020) 1001–1010

Available online at www.sciencedirect.com

Reports of Practical Oncology and Radiotherapy

journal homepage: http://www.elsevier.com/locate/rpor

Original research article

# Validation of Monte carlo Geant4 multithreading code for a 6 MV photon beam of varian linac on the grid computing

Mustapha Assalmi[a,*], El Yamani Diaf[a], Najim Mansour[b]

[a] Physics Team, Lab: OLMAN-RL, Multidisciplinary Faculty of Nador, University Mohammed First Oujda, Morocco
[b] Faculty of Science and Technical, Errachidia, Morocco

ARTICLE INFO

*Article history:*
Received 23 April 2020
Received in revised form 28 July 2020
Accepted 16 September 2020
Available online 12 October 2020

*Keywords:*
Monte carlo
Grid computing
Dose
Medical accelerator
Photon beams
Geant4
G4Linac-MT
Multithreaded

ABSTRACT

*Aim:* To evaluate the computation time efficiency of the multithreaded code (G4Linac-MT) in the dosimetry application, using the high performance of the HPC-Marwan grid to determine with high accuracy the initial parameters of the 6 MV photon beam of Varian CLINAC 2100C.
*Background:* The difficulty of Monte Carlo methods is the long computation time, this is one of the disadvantages of the Monte Carlo methods.
*Materials and methods:* Calculations are performed by the multithreaded code G4Linac-MT and Geant4.10.04.p02 using the HPC-Marwan computing grid to evaluate the computing speed for each code. The multithreaded version is tested in several CPUs to evaluate the computing speed according to the number of CPUs used. The results were compared to the measurements using different types of comparisons, $TPR_{20,10}$, penumbra, mean dose error and gamma index.
*Results:* The results obtained for this work indicate a much higher computing time saving for the G4Linac-MT version compared to the Geant4.10.04 version, the computing time decreases with the number of CPUs used, can reach about 12 times if 64CPUs are used. After optimization of the initial electron beam parameters, the results of the dose simulations obtained for this work are in very good agreement with the experimental measurements with a mean dose error of up to 0.41% on the PDDs and 1.79% on the lateral dose.
*Conclusions:* The gain in computation time leads us to perform Monte Carlo simulations with a large number of events which gives a high accuracy of the dosimetry results obtained in this work.


## 1. Background

External radiotherapy is the most common technique for the treatment of tumours. This method of treatment consists of delivering a precise dose of ionising radiation into a tumour volume, while preserving the surrounding healthy tissue as much as possible. Ionizing radiation is produced in the form of beams of varying size and energy by linear particle accelerators located at a distance from the patient. The radiation beam reaches the tumour by passing through the patient's skin to deliver the dose necessary to destroy the tumour cells. Developments in external radiotherapy have led to an improvement in the calculation of the absorbed dose in a medium. Monte Carlo calculations are now available in clinical settings to simulate the dose distribution in a volume.

In this work, the medical linear accelerator used is the Varian Clinac 2100C at the Hassan II Oncology Centre in Oujda, Morocco, for a photon beam of 6 MV energy and configured in different irradiation fields of $10 \times 10\,cm^2$, $15 \times 15\,cm^2$ and $20 \times 20\,cm^2$. Different codes based

on Monte Carlo methods are used by many scientific researchers to accurately simulate complex geometry in order to study the interaction of radiation with matter and particle transport. In the present work, the modelling of the LINAC geometry to simulate the dose distribution has been reproduced on the basis of the Monte Carlo Geant4 (Geometry And Tracking) method. The Geant4 Simulation Toolkit was first used in 1994 in a research project for a new general purpose simulation code for high energy physics.[1] The GEANT4 Monte Carlo particle transport simulation code is widely used in medical physics,[2] this code has some advantages over other codes such as EGSNRC, XVMC, MCNP, PENELOPE and FLUKA as indicated by different authors.[1] Geant4 can handle all types of particles, is capable of handling complex geometries and offers the most flexible geometry description among all Monte

* Corresponding author.
*E-mail addresses:* m.assalmi@ump.ac.ma (M. Assalmi), eldiaf@gmail.com (E.Y. Diaf).

https://doi.org/10.1016/j.rpor.2020.09.011
1507-1367/

Carlo codes. The difficulty of Monte Carlo methods is the long computing time that varies according to the type of code and the performance of the machines used in the simulations, now with the development of computer technology offers virtual computing grids that allow to make distributed calculations exploiting the computing power (processors, memories . . .) of thousands of computers to give the illusion of a very powerful virtual computer. This model allows to solve important calculation problems requiring very long execution times. For this work all the calculations of simulations are made thanks to the HPC-Marwan grid which offers us a high performance of calculation. In this study, we investigated the computing time savings consumed by Monte Carlo simulation on different CPUs for the standard version of Geant4.10.04 and the multithreaded version G4Linac-MT, using distributed computing of the HPC-Marwan grid. The percentage of the depth dose (PDD) and the beam profile were calculated in a $40 \times 40 \times 40\,cm^3$ water phantom and compared to those measured using the gamma index comparison method,[3] $TPR_{20,10}$, penumbra and error estimators.[4] The analysis of the results is done using the ROOT data analysis platform.[5]

## 2. Aim

The aim of this study is to reduce the computation time in Monte Carlo simulations, with the evaluation of the computation time efficiency of the multithreaded code (G4Linac-MT) in dosimetry application, using the HPC-Marwan grid, the latter allowed us to achieve high performance computing with 192 CPUs per user. The multithreaded code (G4Linac-MT) is applied to determine the initial parameters (mean energy, sigma and beam width of the incident electron in the tungsten target) of the 6 MV photon beam of Varian Clinac 2100C with high accuracy justified by different types of comparisons.

## 3. Materials and method

### 3.1. LINAC head modelling

We modelled the geometry of the treatment head of the Varian Clinac 2100C linear accelerator by Monte Carlo simulation using the geometry script language provided by the Geant4 simulation toolkit, and saved it in a text file with a" .geom" extension for G4Linac-MT[6] and using the C++ language" ML2Acc1.cc" for Geant4.10.04.[2,7] Fig. 1 is illustrated using the Hep-RApp visualization tool. The model consists primarily of the tungsten X-ray target with a copper layer placed under the target to absorb low-energy electrons, the 7.6 cm thick primary collimator, and the copper flattening filter attached to the lower end of a beryllium window, the latter has the shape of a thin cylinder, it has been modelled at the exit of the primary collimator, their role is to filter low energy X-rays, an ionization chamber, a mirror inclined at an angle of 35° and secondary collimators formed by the upper (Y) and lower (X) jaws.

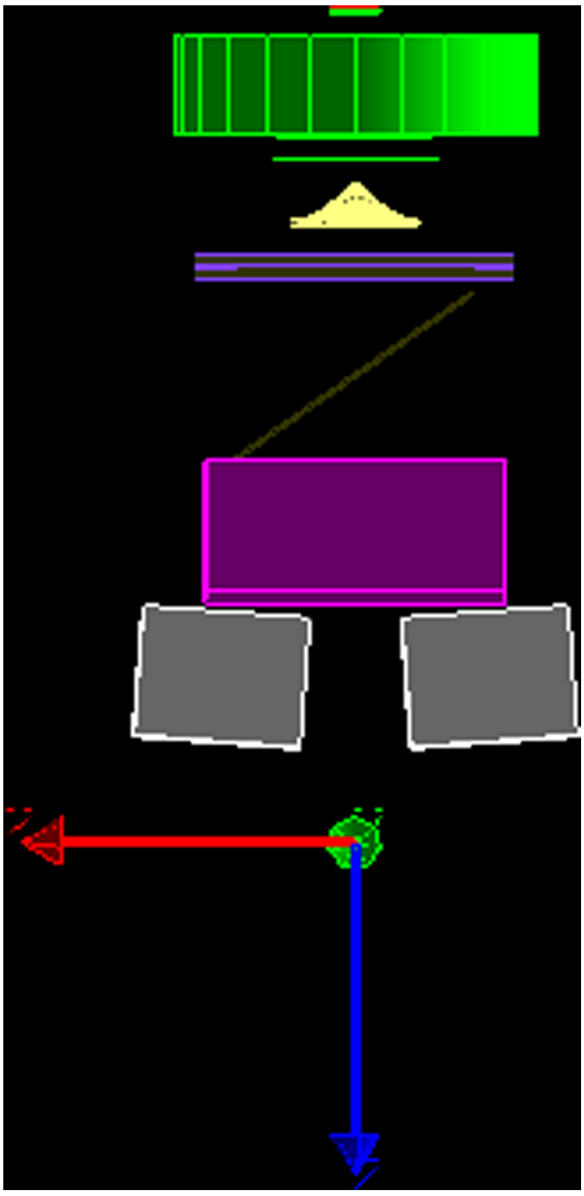

**Fig. 1.** Visualization of Linac Varian 2100C treatment head geometry by means of HeppRep visualization system.

**Table 1**
Comparison of the calculation time of G4Linac-MT and Geant4.10.04 codes.

| | Geant4.10.04 | | G4Linac-MT(64CPUs) |
|---|---|---|---|
| Particle source used | Target | Phase space | Phase space |
| Primary electrons | $10^8$ | $10^8$ | $10^8$ |
| No. of histories | $10^7$ | $10^7$ | $10^7$ |
| Times of calculs (days) | 54 | 3.57 | 0.28 |

### 3.2. Monte Carlo simulations

Among the disadvantages of Monte Carlo methods is the time required for the calculation, the precision of the calculation increases with the increase in the number of simulated histories ( number of events executed to score the dose in a water phantom),[8] in this work the HPC-Marwan computing grid is used for all the simulation calculations. A test is made in this study on both versions of Geant4 based on the computing time to save the maximum possible time thanks to the high performance of the computing grid. Table1 shows the number of primary electrons generated and simulated histories as a function of time, using two versions of Geant4, version 10.04p02 and version G4Linac-MT (Geant4-based code for Linac modelling with Multithreading support) based on Geant4.10.05. To optimize the computation time we created a phase space plane with a thickness of 0.02 mm placed at SSD = 100 cm as a source to simulate the dose distribution in the phantom, which collects dataset specifying the position, the direction, the energy, the type and additional particle variables for each particle generated from the initial source crossing the phase space plane. The phase space file format for G4Linac-MT is based on HDF5 C++ scientific library, it stores meaningful data related to all particles reaching a defined

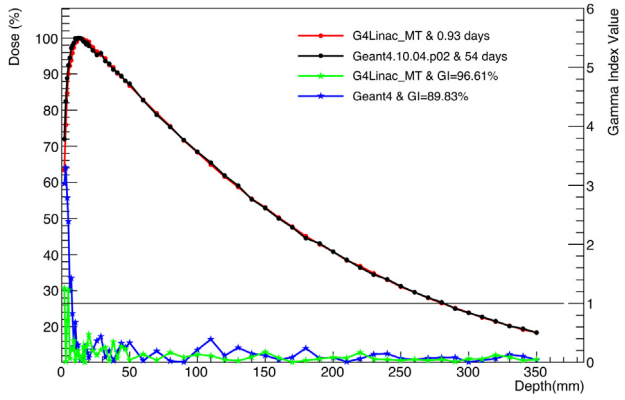


**Fig. 2.** Comparison of dose depth calculation time for G4Linac_MT and Geant4.10.04.p02 codes configured under the same initial conditions.

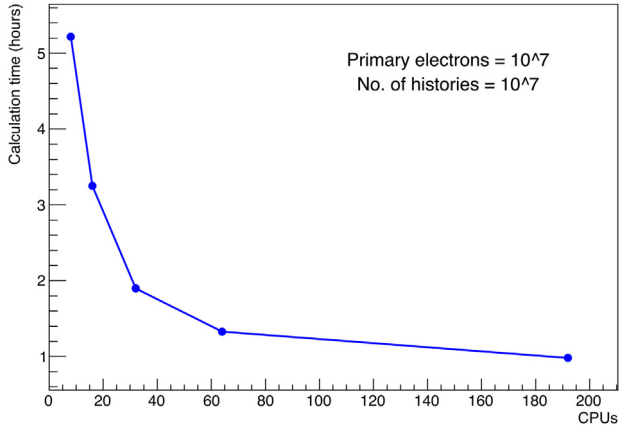


**Fig. 3.** Calculation time of the G4Linac-MT code on various CPUs.

Z-coordinate of a plane crossed by a linac beam, and an ASCII file format for Geant4.10.04 presents as a text file whose data is encoded as a series of text columns. In order to have an agreement of the dose calculations with the measured dose it is necessary to increase the number of histories, in Figs. 2 the number of histories has been increased to $10^8$ for the G4Linac-MT code (calculation time is carried in 0.93 days ) and the dose calculated in 54 days for the Geant4.10.04, the two codes are configured in the same initial conditions, the result is shown in Fig. 2 with the result of the gamma index compared to the experimental result for each code, the gamma index is set to 2 mm/2% indicate that the accuracy of dose calculation is increased with the increase in the number of simulated histories.

The calculation debit for the code Geant4.10.04 does not depend on the number of CPUs, this code is tested on a different number of CPUs and has no influence on the execution time, on the other hand the code G4Linac-MT depends strongly on the number of CPUs used. The computation time decreases with the increasing number of CPUs for the Multithresds version, Fig. 3 explains the variation in computing time for the multithreading version (G4Linac-MT) depending on the CPUs, the computing time is counted for 8, 16, 32, 64 and 192 CPUs.

### 3.3. Monte Carlo validation

The MC calculations were combined with clinical results measured in a water phantom for the 6 MV X-ray energy using Varian Clinac 2100 (Varian Oncology Systems, Palo Alto, CA, USA) accelerator at the Hassan II oujda oncology centre measured on September 12, 2019. Data acquisition was performed with 31,021 Semiflex 3D chamber (PTW, Freiburg, Germany), it is a waterproof cylindrical chamber has 0.07cm$^3$ in volume. The measurements were carried out into the water phantom (PTW BEAM SCAN) equipped with water detector. MEPHYSTO software was used for data acquisition and analysis. The comparisons between calculated and measured dose results were normalized to the maximum dose, the simulation calculations were evaluated by calculating the mean point-to-point dose error[4] with the following equation:

$$\varepsilon = \frac{1}{N}\sum_i \left( \frac{\left|(Dc_i - Dm_i)\right|}{Dm_i} \right) x100$$

$\varepsilon$ is the mean point-to-point error, i corresponds to a curve point index, N is the number of points, $Dc_i$ is the dose calculated at point i and $Dm_i$ is the reference dose measured at point i.

Other comparisons were made using gamma indices[3] to evaluate the simulation calculations with a criterion of 2%/2 mm, the accuracy proposed by Chetty et al.[9] The gamma index method allows the comparison of two distributions, the measured dose is considered as the reference distribution and the calculated dose is the distribution to be evaluated. An ellipse belonging to the reference distribution is defined around each point. When 100% of the points pass the 2%/2 mm criterion, this means that all points have passed the comparison. The explanation of gamma index is also presented in detail in the publication Physica Medica 36 (2017) 1–11.[10]

After determining the initial parameters using the gamma index and the mean dose error, we evaluated the dose distribution (percent depth dose (PDD) and beam profile) for different field sizes and dose profiles for 3 depths, all dose calculations were validated by experimental data. The simulations were performed for square field sizes of $10 \times 10$, $15 \times 15$ and $20 \times 20$ cm$^2$ and the beam profile for different depths of 1.5, 10, and 20 cm in homogeneous phantom water of size $40 \times 40 \times 40$ cm$^3$, placed at SSD = 100 cm.

### 3.4. Grid computing methodology

Due to the high computing time for Monte Carlo calculations which is one of the most important obstacles for the application of Monte Carlo code to clinical practice for dose distribution calculation, the HPC-MARWAN - CNRST computing grid[11,12] is used to reduce the execution time of the Geant4 code. The HPC-MARWAN cluster is composed of 19 nodes managed by the National Center for Scientific and Technical Research / Rabat (CNRST) and offers the following capacities: 760 cores (68 TFlops), 5.2 TB of memory, 108 TB of storage, 2 GPU cards. These nodes are interconnected by a very low latency network (OPA) at 100 Gbps, which optimizes performance for parallel computing. This infrastructure is connected to the MARWAN network by a 5 Gbps link which ensures a fluidity in the use and transfer of data from the Univer- sities.[13]

The job management tool is SLURM (Simple Linux Utility for Resource Management) is an open source, fault-tolerant, and highly scalable cluster management and job scheduling system for large and small Linux clusters. Slurm requires no kernel modifications for its operation and is relatively self-contained. As a cluster workload manager, Slurm has three key functions. First, it allocates exclusive and/or non-exclusive access to resources (compute nodes) to users for some duration of time so they can perform work. Second, it provides a framework for starting, executing, and monitoring work (normally a parallel job) on the set of allocated nodes. Finally, it arbitrates contention for resources by managing a queue of pending work.[14] The development of SLURM began in 2002 at the Lawrence Livermore Laboratory (USA) as a resource manager for Linux clusters. The architecture of the Slurm is shown in Fig. 4.

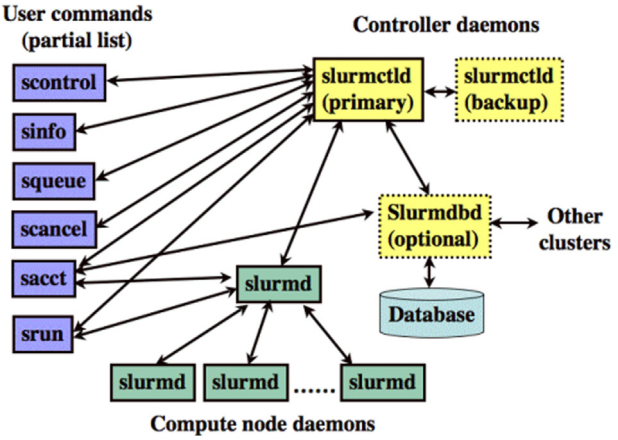


**Fig. 4.** Slurm components.

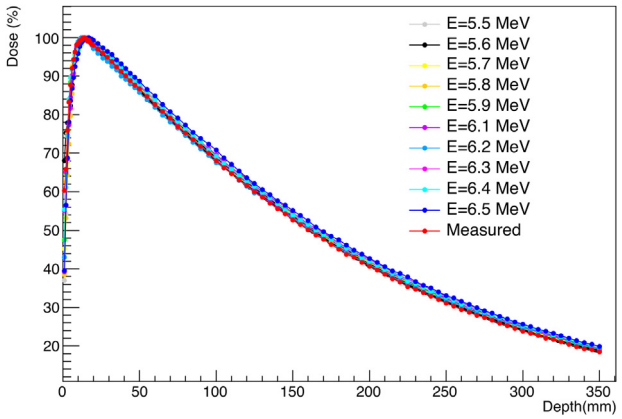


**Fig. 6.** Comparison of dose distribution PDD curves calculated for various mean energy of 6 MV photon beam for $15 \times 15\,cm^2$ field.

The submission of a job on the computing grid is necessary to write a command script, defines the components of a job, the requested resources (defined in resource blocks called Tasks) and the different steps of the job. Job steps are executed sequentially or in parallel, they create one or more Tasks (executed in parallel) and manage the distribution of allocated resources. In Fig. 5, the SBATCH options define the name of the job, the partition used, the number of Tasks (–ntasks) and the number of CPUs per Task (–cpus-per-task ), the allocation will then be 64 CPUs. The execution of the Batch" script.slurm" is launched via the" sbatch" command.

## 4. Results

### 4.1. Estimation of mean energy

We have simulated the depth dose distribution for different energies from 5.5–6.5 MeV with a step size of 0.1 MeV for the irradiation field of $15 \times 15\,cm^2$, in a phantom of 40 cm at these dimensions, the depth dose is calculated in 90 voxels of size $0.5 \times 0.5 \times 0.1\,cm^3$. For this part, we have fixed the focal spot = 1 mm and the sigma energy in 0.5 MeV. For all PDDs, the initial number of simulated electrons is $10^8$ and the number of simulated histories is $2.10^8$. Fig. 6 shows the PDD obtained for different simulated energies and compares it to the measured dose.

**Table 2**
Gamma Index tests and error estimators result from testing mean energy of the electron beam.

| Energy (MeV) Energy (MeV) | Error estimators(%) | Gamma Index<1(%) | Gamma Index<0.5(%) |
|---|---|---|---|
| 5.5 | 2.39 | 91.11 | 81.11 |
| 5.6 | 1.53 | 94.44 | 92.22 |
| 5.7 | 2.29 | 95.56 | 55.56 |
| 5.8 | 2.77 | 91.11 | 80.00 |
| 5.9 | 2.50 | 97.78 | 43.33 |
| 6.1 | 2.68 | 94.44 | 58.89 |
| 6.2 | 1.76 | 97.78 | 87.78 |
| 6.3 | 3.50 | 92.22 | 23.33 |
| 6.4 | 3.03 | 97.78 | 18.89 |
| 6.5 | 4.86 | 47.78 | 6.67 |

The difference between the dose distributions calculated by the G4Linac-MT simulation and the clinical measurement in water is analyzed using error estimators and gamma index criteria with a criterion of 2%/2 mm, as shown in Table 2.

The mean energy of the electron beam is very sensitive on the number of brumshtralung photons and consequently on the absorbed dose; Fig. 7 illustrates the photon spectrum with the size of the phasespace in GB for each simulated energy.

The energy spectrum of the photon beam is characterized by three parameters: the maximum energy, the most probable energy

```
#!/bin/bash
#SBATCH --job-name=TestJob          # Job name
#SBATCH --ntasks=1                  # Number of Tasks
#SBATCH --cpus-per-task=64          # Allocation of 64 CPUs by Task
#SBATCH --partition=mediumq         # Name of the partition Slurm used: 2h, 24h, 7d, infinite

#SBATCH -o %x-%j.out
#SBATCH -e %x-%j.err

#============load modules=================================================
module load geant4/gcc/64/mt-4.10.04.p03
module load cmake/gcc/64/3.12.3
module load hdf5_18/1.8.20

#=========== set OMP_NUM_THREADS=========================================

  if [ -n "$SLURM_CPUS_PER_TASK" ]; then
    omp_threads=$SLURM_CPUS_PER_TASK
  else
    omp_threads=1
  fi
export OMP_NUM_THREADS=$omp_threads

#============command compilation/execution================================
```

**Fig. 5.** The Slurm script used to submit a Job on the HPC-Marwan grid.

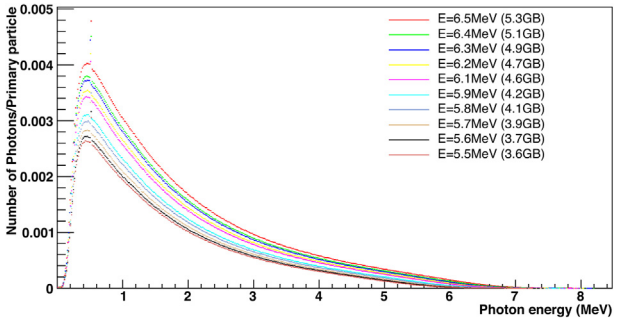


**Fig. 7.** Comparison of photon beams spectrum for various mean energy.

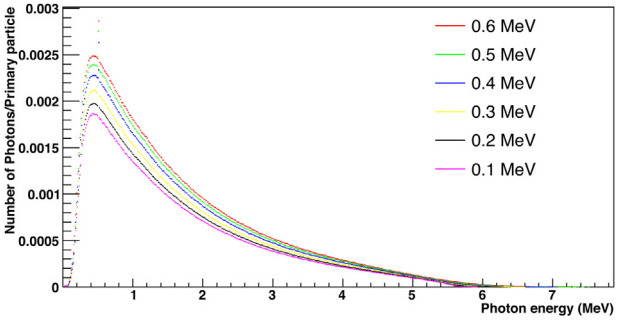


**Fig. 9.** Comparison of photon beams spectrum for various energetic sigma.

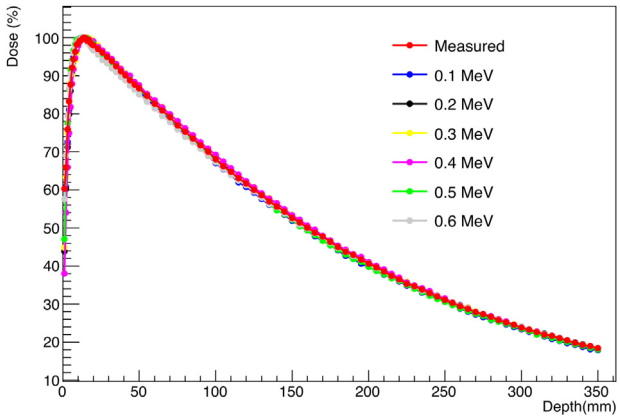


**Fig. 8.** Comparison of dose distribution PDD curves calculated for various energetic sigma of 6 MV photon beam for $15 \times 15\,cm^2$ field.

and the average energy. The average energy value of the spectrum is considered a significant quantity in the calculations of the clinical increase of the TPS dose. According to the results obtained for the ten energies tested for the 6 MV photon beam, gamma index tests (Table 2) showed that the best agreement between the measured and simulated values is obtained for the mean energy of 5.6 MeV. Indeed, for this configuration indicates an estimation error of 1.53% and 94.44% of the calculated points are less than 1 with an accuracy of 2 mm/2% for the depth dose curve.

### 4.2. Estimation of energetic sigma

We considered in a second time to take the mean energy of 5.6 MeV as a starting configuration for the second study and fixed the focal spot in 1 mm, then we are looking to optimize the parameters related to the Gaussian energy distribution, this by varying the energy sigma considering six sigma values ranging from 0.1 MeV to 0.6 MeV with a step of 0.1 MeV. The depth dose distributions were calculated in the homogeneous water phantom irradiated at a field of $15 \times 15\,cm^2$ at a distance of 100 cm between the target and the phantom surface. Fig. 8 illustrates the comparison of the dose PDDs obtained for the different energy sigma values and compares them to the measured dose.

Monte Carlo simulation calculations are compared with measured data and analyzed using error estimators and gamma index criteria with an accuracy of 2 mm/2%. The results of the gamma index tests for depth fields for the different energy sigma values are summarized in Table 3.

To detail the influence of the Gaussian energy distribution on the absorbed dose, Fig. 9 shows the spectrum of the brumschtralung photons for each Gaussian energy. From the results obtained for the tested sigma values of the 6 MV photon beam, the gamma indices (Table 3) showed that the best agreement between the measured and simulated values is obtained for the 0.2 MeV energy sigma value. Indeed, for this configuration indicates a dose error of 1.03% and 95.56% of the calculated points passing $\gamma < 1$ in all region of PDD and 100% passing $\gamma < 0.5$ in region $Z < Z_{dmx}$ with an accuracy of 2 mm/2%.

### 4.3. Estimation of the beam width

A third study was conducted to evaluate the effect of focal spot size variation on calculated dose distributions in a water phantom. This was done by varying the focal spot size from 0.6 mm to 1.3 mm with a 0.1 mm step size. The direction of the photons produced by the interaction of the electrons with the target is obtained from the angular distribution of the Bremsstrahlung irradiation head.[15] Fig. 11 shows the effect of the electron beam width on the angular distribution of the 6 MV Bremsstrahlung photons with the mean photon energy in phase space for each focal spot. The photon beam is structured from the results of the previous configurations, in which the mean energy and the Gaussian energy distribution of the electron beam are fixed at 5.6 MeV and 0.2 MeV, respectively. The calculations are performed for a square field of $15 \times 15\,cm^2$ and a surface distance of 100 cm. The depth dose Fig. 10 is compared with the measured data and the difference between them is analyzed using the gamma index and mean dose error criteria. Table 4 summarizes the gamma index and mean dose error for each width of the electron beam.

From Fig. 11, we can see that the difference between the curves of the angular distribution of the bremshtrahlung photons is quite small as a function of the electron beam width, we observe that the mean energy of the bremshtrahlung photons varies from 6.98 keV between 0.6 mm and 1.3 mm of the electron beam widths. The dose distributions were calculated in a homogeneous water phantom

**Table 3**
Gamma Index tests and error estimators result from testing energetic sigma of the electron beam.

| % | 0.1MeV | 0.2MeV | 0.3MeV | 0.4MeV | 0.5 MeV | 0.6MeV |
|---|---|---|---|---|---|---|
| Error | 1.88 | 1.03 | 1.05 | 1.80 | 1.50 | 0.98 |
| G.Index<1 | 95.56 | 95.56 | 94.44 | 92.22 | 94.44 | 94.44 |
| G.Index<0.5 | 86.67 | 93.33 | 92.22 | 84.44 | 88.89 | 70.00 |
| $Z < Z_{dmx}$(GI < 0.5) | 71.43 | 57.14 | 57.14 | 35.71 | 42.86 | 50.00 |
| $Z > Z_{dmx}$(GI < 0.5) | 89.47 | 100.00 | 98.68 | 93.42 | 97.37 | 73.68 |

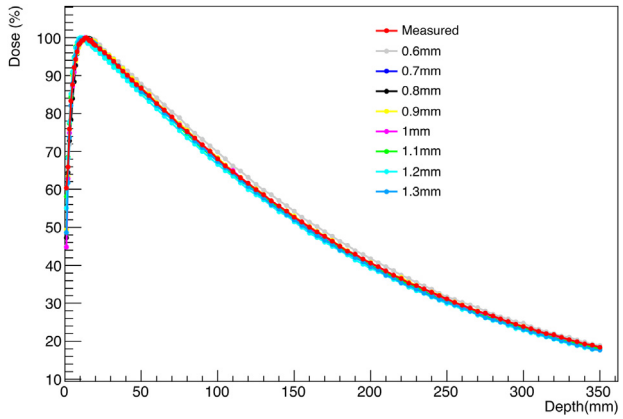


**Fig. 10.** Comparison of dose distribution PDD curves calculated for various beam widths of 6 MV photon beam for $15 \times 15\,cm^2$ field.

**Table 4**
Gamma index tests and error estimators result from each focal spot.

| Focal spot size(mm) | Error estimators(%) | Gamma Index<1 (%) | Gamma Index<0.5 (%) |
|---|---|---|---|
| 0.6 | 2.27 | 95.56 | 50.00 |
| 0.7 | 1.59 | 92.22 | 90.00 |
| 0.8 | 1.20 | 94.44 | 92.22 |
| 0.9 | 0.64 | 96.67 | 95.56 |
| 1 | 1.03 | 95.56 | 93.33 |
| 1.1 | 1.60 | 93.33 | 86.67 |
| 1.2 | 2.80 | 93.33 | 16.67 |
| 1.3 | 1.95 | 96.67 | 83.33 |

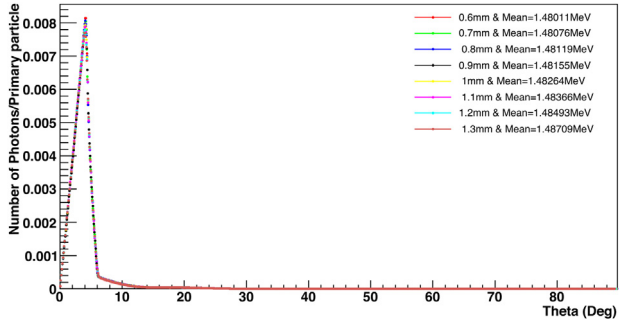


**Fig. 11.** Comparison of the angular distribution of photons for each focal spot size.

irradiated in a field of $15 \times 15\,cm^2$. Based on the results presented in Table 4, identifying the electron beam width, it can be said that the absorbed dose in a volume is very sensitive to variation in the electron beam width, as shown in Fig. 10. Based on the results of the gamma index and estimation error for dose calculations, showed good agreement between the MC calculations and those measured when the FWHM is set at 0.9 mm.

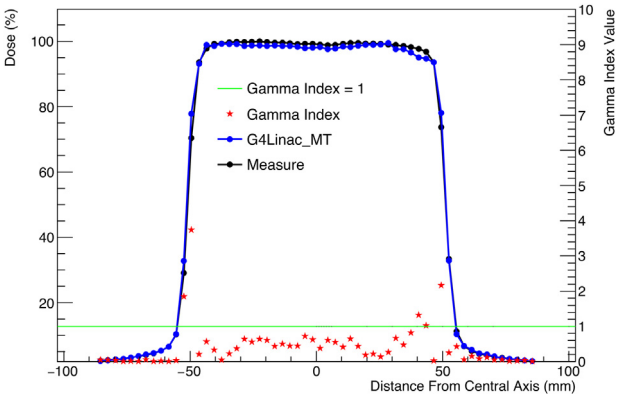


**Fig. 12.** Depth of 1.5 cm for $10 \times 10\,cm^2$ field size.

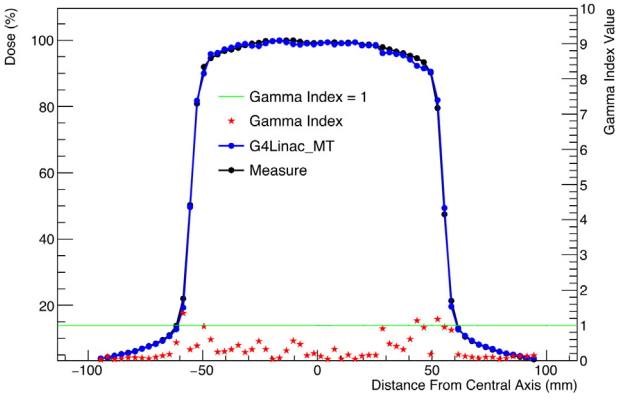


**Fig. 13.** Depth of 10 cm for $10 \times 10\,cm^2$ field size.

The results obtained from the initial parameters of the 6 MV photon beam compared with those found in previous studies by different MC codes and different Linac types have been summarized in Table 5. Thus, we can say that the G4Linac-MT model of the Varian Clinac 2100C medical accelerator at the Hassan II Oncology Center in Oujda, Morocco is accurately simulated and the initial electron beam parameters have been accurately determined.

### 4.4. Dose profiles comparison

After determination of the initial electron beam parameters, the validation of the lateral dose results of the Monte Carlo simulation using the multithreaded version G4Linac-MT code is presented in Figs. 12–20. The deposited doses were calculated in a homogeneous water phantom with external dimensions of $40 \times 40 \times 40\,cm^3$, the calculations are performed for irradiation fields of $10 \times 10$, $15 \times 15$ and $20 \times 20\,cm^2$ and at three depths of 1.5, 10 and 20 cm at a distance of 100 cm between the target and the phantom surface. The

**Table 5**
Comparison of initial electron beam parameters with different types of codes and linacs.

| Energy (MeV Energy (MeV | FWHM(MeV) | FWHM(mm) | Linac Type | Code Type | Authors |
|---|---|---|---|---|---|
| 5.3 | – | 3.6 | Varian 2100C | BEAMnrc | [16] |
| 5.95 | 0.2 | 1.2 | Varian clinaciX | PRIMO | [17] |
| 6.52 | | 1.4 | Varian 2100C | BEAMnrc | [18] |
| 5.6 | 0.42 | 1.177 | Varian 2100C | Geant4.9.4 | [19] |
| 5.6 | | 2.5 | Varian 2100C | BEAMnrc | [20] |
| 5.8 | 0.174 | 3 | Elekta Precise | GATE | [4] |
| 5.9 | 0.8268 | 2.5 | Varian 2300IX | Geant4.9.6 | [21] |
| 6 | 0.127 | 0.5 | Varian 600C | Geant4.9.5 | [22] |
| 5.6 | 0.2 | 0.9 | Varian 2100C | G4Linac_MT | This study |

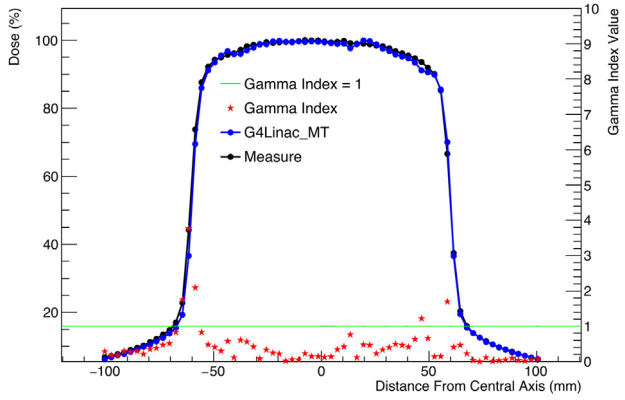


**Fig. 14.** Depth of 20 cm for $10 \times 10\,cm^2$ field size.

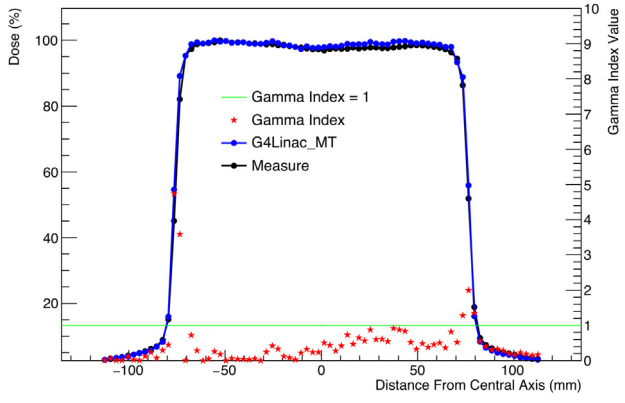


**Fig. 15.** Depth of 1.5 cm for $15 \times 15\,cm^2$ field size.

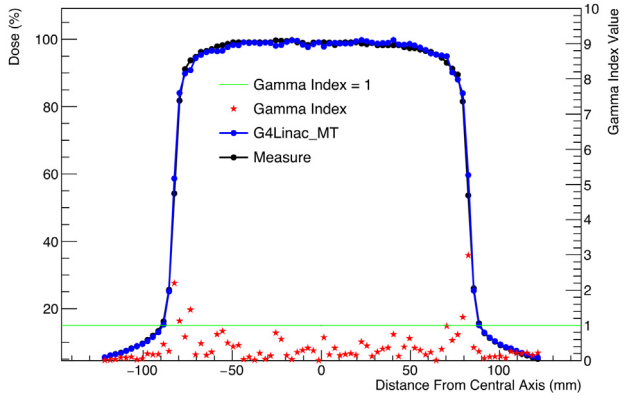


**Fig. 16.** Depth of 10 cm for $15 \times 15\,cm^2$ field size.

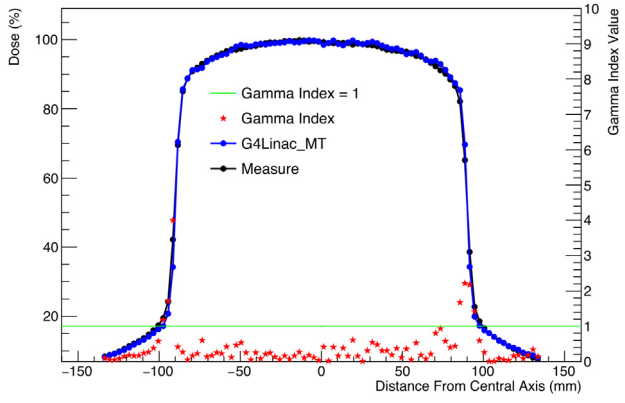


**Fig. 17.** Depth of 20 cm for $15 \times 15\,cm^2$ field size.

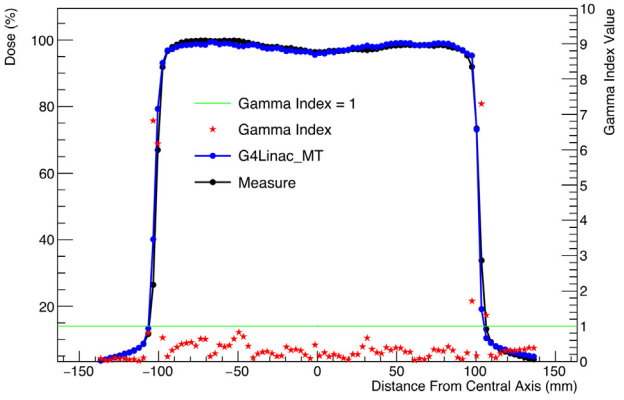


**Fig. 18.** Depth of 1.5 cm for $20 \times 20\,cm^2$ field size.

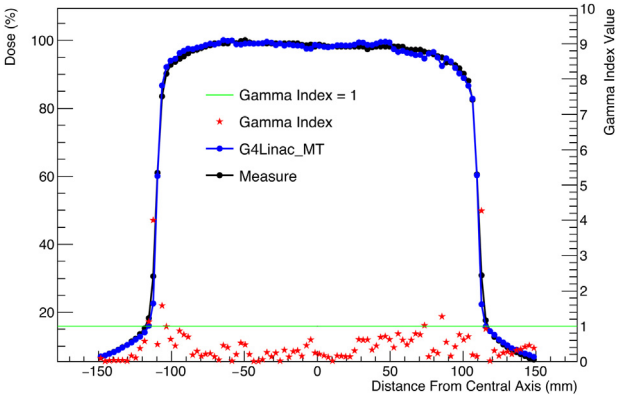


**Fig. 19.** Depth of 10 cm for $20 \times 20\,cm^2$ field size.

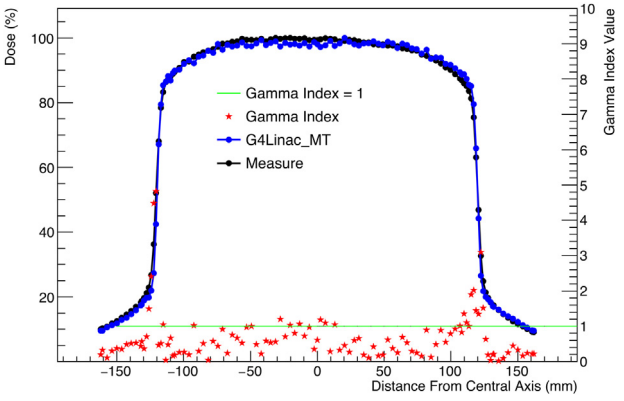


**Fig. 20.** Depth of 20 cm for $20 \times 20\,cm^2$ field size.

size of the simulated voxels is chosen to $0.3 \times 0.5 \times 0.5\,cm^3$. The phase space file is about 4 GB for an initial number of simulated electrons of $10^8$, for this part we increased the number of histories to $2.10^9$ to obtain an excellent statistical uncertainty in the lateral distribution of the dose. the calculated and measured dose profiles are normalized to the maximum value as follows :

$$Relativedose\,(\%) = \frac{D_i}{D_{max}}$$

where $D_i$ is the dose at any position; and $D_{max}$ is the dose maximum. The dose profile curves are divided into three regions. The first is an inner field where the area is covered by the open field of the jaws, the second is the penumbra where the dose falls rapidly at the edge of the beam, and the third is an outer field where the area is not covered by the open field of the jaws.[23] We use differ-

**Table 6**
Gamma index values, error estimators and Penumbra for beam profile in different field sizes.

| Field ($cm^2$) | Depth (cm) | Gamma index(%) | | | | Error (%) | Penumbra (mm) | |
|---|---|---|---|---|---|---|---|---|
| | | <1 | <0.5 | | | Measured | Simulated | |
| | 1.5 | 91.38 | 68.97 | 2.04 | 2.07 | 2.51 | 5.76 | 5.08 |
| 10 × 10 | 10 | 95.31 | 79.69 | | | | 6.62 | 6.78 |
| | 20 | 92.65 | 79.41 | | | | 8.38 | 7.83 |
| | 1.5 | 93.42 | 72.37 | 3.19 | 1.79 | 2.07 | 5.34 | 4.90 |
| 15 × 15 | 10 | 93.90 | 78.05 | | | | 7.58 | 7.07 |
| | 20 | 92.22 | 81.11 | | | | 10.55 | 7.95 |
| | 1.5 | 94.57 | 83.70 | 3.55 | 2.42 | 3.05 | 5.88 | 5.40 |
| 20 × 20 | 10 | 94.00 | 70.00 | | | | 8.12 | 6.69 |
| | 20 | 79.82 | 48.62 | | | | 11.80 | 9.26 |

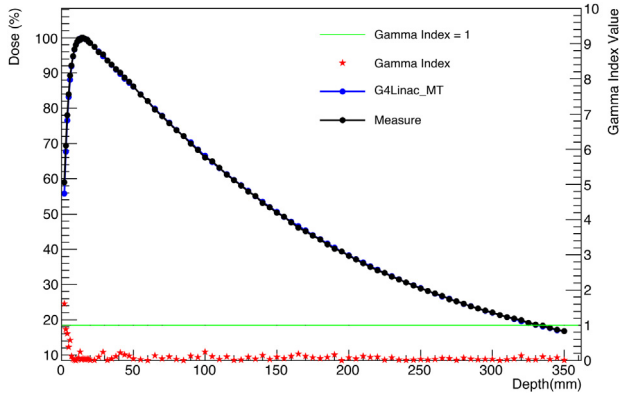


**Fig. 21.** PDD for the 10 × 10 $cm^2$ field size.

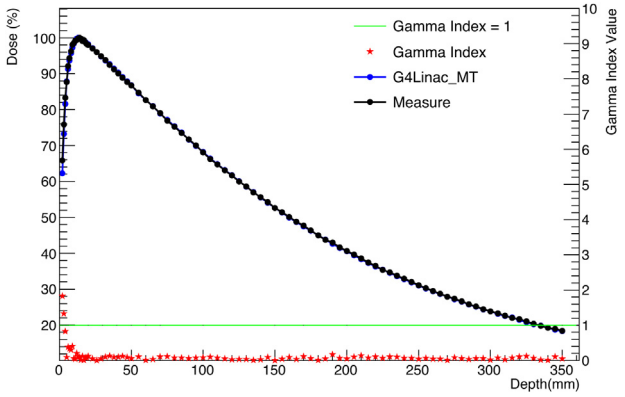


**Fig. 22.** PDD for the 15 × 15 $cm^2$ field size.

ent types of analysis of the simulation results in comparison with the clinical measurement of the Varian Clinac 2100C accelerator at the Hassan II Oncology Centre in Oujda, Table 6 shows the analysis results obtained. The analysis is based on the values of gamma index and mean dose error and the penumbra.

The physical penumbra width is defined as the lateral distance from the central axis between 20% and 80% of the central axis dose at a reference depth.[24]

Analysis of the difference between the dose profile calculated using the G4Linac-MT code and the experimental result showed excellent agreement with a mean dose error below 3.55% for the 9 calculations shown in Table 6. The area of the penumbra that has high error in the Monte Carlo calculations, as shown by the gamma index values in Fig. 12–20. From the penumbra results in Table 6, the large penumbra difference is 2.6 mm is observed for the 20 × 20 $cm^2$ field at 20 cm depth and the short difference of 0.16 mm is observed for the 10 × 10 $cm^2$ field at 10 cm depth.

### 4.5. Depth dose comparison

The depth dose distribution calculated by monte carlo simulations of the multithreaded version G4Linac-MT is also evaluated based on the initially determined parameters. The dose calculations are performed for three irradiation fields 10 × 10, 15 × 15 and 20 × 20 $cm^2$ for a homogeneous water phantom of 40 × 40 × 40 $cm^3$ in these dimensions. The voxelized phantom size were 0.5 cm, 0.5 cm, 0.1 cm, along x, y and z respectively. The number of voxels were 1, 1, 89 along x, y and z respectively. Fig. 21–23 shows the comparison of the simulation results and the experimental results of the depth dose profiles for each field. The depth dose is presented with the relative dose in percent, each dose at a certain point is normalized to the maximum value. The initial number of simulated electrons is of $10^8$ and a $5.10^8$ histories were used for each simulation calculation. The analysis of the simulation results in relation to

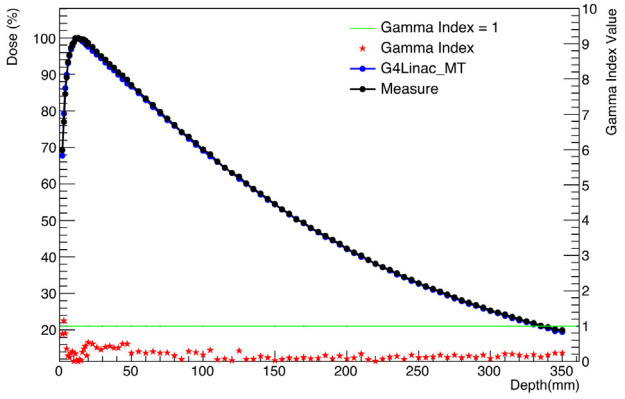


**Fig. 23.** PDD for the 20 × 20 $cm^2$ field size.

the clinical measure is presented in Table 7. In this analysis, we used the values of gamma index, mean dose error and $TPR_{20,10}$ (Tissue Phantom Ratio).

TPR is recommended by most IAEA dosimetry protocols. The TPR values were determined from the measured $PDD_{20\,cm}$ and $PDD_{10\,cm}$ data using an empirical approximation relationship[25,26] :

$$TPR_{20,10} = 1.2661 \times PDD_{20,10} - 0.0595$$

where $PDD_{20,10}$ is the ratio of doses as a percentage of depth at 20 cm and 10 cm depth.

As shown in Table 7, the results obtained show a better correspondence between the Monte Carlo simulations of the G4Linac-MT code and the experimental depth dose measurements with an mean dose error below 0.76% for the three irradiation fields 10 × 10, 15 × 15 and 20 × 20 $cm^2$. According to Figs. 21–23, the gamma index is higher in the build-up region, dose errors were observed at 10 cm depth of 0.47%, 0.51% and 0.72%, for fields of

**Table 7**
Gamma index values, error estimators and $TPR_{20,10}$ for PDD in different field sizes.

| Field($cm^2$) | Gamma index(%) | | | | | Error(%) | | $TPR_{20,10}$ | |
|---|---|---|---|---|---|---|---|---|---|
| | < 1 | < 0.5 | | | | Measured | | Simulated | |
| 10 × 10 | 98.88 | 95.51 | 0.41 | 0.43 | 0.76 | 0.671 | 0.695 | 0.712 | 0.669 |
| 15 × 15 | 97.75 | 96.63 | | | | | | | 0.696 |
| 20 × 20 | 98.88 | 95.51 | | | | | | | 0.713 |

**Table 8**
Comparison of the $TPR_{20,10}$ value to that found by other studies of Linac Varian 2100C.

| | Ashokkumaret al.,2017[28] | Beyer, 2013[29] | IAEA[25] | This study |
|---|---|---|---|---|
| $TPR_{20,10}$ | 0.670 | 0.667 | 0.6694 ± 0.0040 | 0.669 |

10 × 10, 15 × 15 and 20 × 20 $cm^2$ respectively. The dose differences in this region obtained in this study are in agreement with those obtained by the PRIMO code for 6 MV Varian Clinac iX (B.Sarin et al., 2020).[17] The dose distribution gradient is high in the build-up region because electrons will be ejected when the 6 MeV photon interacts with the water phantom, these electrons will deposit their energy in the water and the production of electrons will decrease with depth inside the water phantom since the photon energy fluence continuously decreased.[23] For a good dose measurement in the build-up region, a fine size ionization chamber (parallel plate ionization chambers) is required,[27] so the choice of a suitable measuring device is important, this is the reason for the large differences in this region, that the Varian 2100C data acquisition were measured at our oncology centre by 31,021 Semiflex 3D chamber (PTW Freiburg, Germany) used for high energy photon fields in absolute and relative dosimetry. It is a waterproof cylindrical chamber, with 0.07 $cm^3$ nominal sensitive volume, 4.8 mm active length and 2.4 mm radius.

As we signed, IAEA recommends $TPR_{20,10}$ as a quality index for all dosimetry protocols. Based on the results obtained for this work (Table 7), it can be said that the geommetry of the Varian Clinac 2100C Medical accelerator was modelled with high accuracy using G4Linac-MT code, which can be confirmed by the $TPR_{20,10}$ values found in other studies on the same machine. Table 8 is a summary of the results obtained from $TPR_{20,10}$ in previous studies for a 6 MV photon beam and 10 × 10 $cm^2$ fields.

## 5. Conclusions

In this work, the geometry of the head of the Varian Clinac 2100C medical linear accelerator was modeled, and the dose simulation calculations were compared with measurements from the Hassan II Oncology Center oujda Morocco. The calculations are performed by G4Linac multithreaded code using the high performance of the HPC-Marwan computing grid. Several aspects should be highlighted in this study:

- A high computation speed for the multithreading version with a gain can reach about 12 times more than Geant4.10.04.p02 if 64 CPUs are used.
- The speed of calculation of the G4Linac-MT code strongly depends on the number of CPUs used, can create a phase space of $10^7$ particles and generate it with $10^7$ histories in 0.98 h if 192 CPUs are used.
- Thanks to the time saved in the calculation with the G4Linac-MT code, more than 25 simulations were performed for a large number of events and generated for a fine precision in determination of the primary electron beam parameters.
- The results obtained in the determination of the initial electron beam parameters were compared with those found in previous studies by different Monte Carlo codes (Geant4, PRIMO, BEAMnrc and GATE) and different types of Linac (Varian 2100C, Varian 2300 IX, Varian 600C and Elekta Precise).

This precision helps us to obtain an excellent agreement between simulation calculations and experimental measurements, which is justified by different types of comparisons, $TPR_{20.10}$, penumbra, mean dose error and gamma index. The flexibility of the G4Linac-MT code and the performances that give us the HPC-Marwan grid have undoubtedly solved the problems of long computation times for Monte Carlo code methods, studies are planned in the near future to model another type of accelerator, Elekta Synergy MLCi2, and development of the G4Linac-MT code in different applications on the DICOM phantom.

## Conflict of interest

None.

## Financial disclosure

None.

## Acknowledgement

This research was supported in part through computational resources of HPC-MARWAN (www.marwan.ma/hpc) provided by the National Center for Scientific and Technical Research (CNRST), Rabat, Morocco.

## References

1. Sardari D, Maleki R, Samavat H, Esmaeeli A. Measurement of depth-dose of linear accelerator and simulation by use of Geant4 computer code. *Rep Pract Oncol Radiother*. 2010;15:64–68.
2. Caccia B, Andenna C, Cirrone GA. MedLinac2: A GEANT4 based software package for radiotherapy. *Ann Ist Super Sanita*. 2010;46(2):173–177.
3. Low DA, Harms WB, Mutic S, Purdy JA. A technique for the quantitative evaluation of dose distributions. *Med Phys*. 1998;25:656–661.
4. Grevillot L, Frisson T, Maneval D, Zahra N, Badel J-N, Sarrut D. Simulation of a 6 MV Elekta Precise Linac photon beam using GATE/GEANT4. *Phys Med Biol*. 2011;56:903–918.
5. ROOT a Data analysis Framework, URL: https://root.cern.ch/.
6. Bakkali J. https://github.com/EL-Bakkali-Jaafar/G4Linac_MT/releases, 2019.
7. The Geant4 web site and Manual, URL: http://geant4.web.cern.ch/.
8. EL Bakkali J, Doudouh A, Mansouri H. Assessment of Monte Carlo Geant4 capabilities in prediction of photon beam dose distribution in a heterogeneous medium. *Phys Med*. 2018;5:1–5.
9. Chetty I, Curran B, Cygler JE, et al. Report of the AAPM task group no. 105: Issues associated with clinical implementation of Monte Carlo-based photon and electron external beam treat ment planning. *Med Phys*. 2007;34:4818–4853.
10. Hussein M, Clark CH, Nisbet A. Challenges in calculation of the gamma index in radiotherapy - towards good practice. *Phys Med*. 2017;36:1–11.
11. CNRST: Centre National pour la Recherche Scientifique et Technique / Rabat - Institut de recherche pour le dveloppement (IRD), URL: https://www.cnrst.ma/index.php/fr/.
12. HPC-Marwan, URL: https://www.marwan.ma/index.php/services/hpc.

13. High Performance Fabrics by Intel, URL: https://www.intel.com/content/www/us/en/products/network-io/high-performance-fabrics.html.
14. Slurm Workload Manager – Documentation, URL : https:/slurm.schedmd.com/.
15. Gonzales D, Cavness B, Williams S. Angular distribution of thick-target bremsstrahlung produced by electrons with initial energies ranging from 10 to 20 keV incident on Ag. *Phys Rev A (Coll Park)*. 2011; 84:052726.
16. Horová S, Judas L. Monte Carlo modelling of clinical accelerator beams and estimation of primary electron beam parameters. *Radioprotection*. 2018;53:61–66.
17. Sarin B, Bindhu B, Saju B, Nair RK. Validation of PRIMO monte carlo model of clinac R ix 6mv photon beam. *J Med Phys*. 2020;45:24.
18. Bencheikh M, Maghnouj A, Tajmouati J, Didi A. Study of photon beam dosimetry quality for removing flattening filter linac configuration. *Physics AUC*. 2017;27:50–60.
19. EL Bakkali J, EL Bardouni T. Validation of Monte Carlo Geant4 code for a 6 MV varian linac. *J. King Saud Univ. - Sci*. 2017;29:106–113.
20. Mohammed M, El Bardouni T, Chakir E, Boukhal H, Saeed M, Ahmed A-A. Monte Carlo simulation of Varian Linac for 6 MV photon beam with BEAMnrc code. *Radiat. Phys. Chem*. 2018;144:69–75.
21. Park H, Choi HJ, Kim J-I, Min CH. Analysis of dose distribution according to the initial Electron beam of the linear accelerator: A monte carlo study. *J. Radiat. Prot. Res*. 2018;43:10–19.
22. Salama E, Ali AS, Khaled NE, Radi A. Therapeutic dose simulation of a 6 MV Varian Linac photon beam using GEANT4. *J Instrum*. 2015;10:T10008.
23. Arif Efendi M, Funsian A, Chittrakarn T, Bhongsuwan T. Monte carlo simulation of 6 MV flattening filter free photon beam of true beam STx LINAC at Songklanagarind Hospital. *Sains Malays*. 2017;46:1407–1411.
24. Tang SQ, Jen YM, Wu JM. An empirical model for describing the small field penumbra in radiation therapy. *Biomed Res Int*. 2019;2019:7584743.
25. Vargas Castrillón S, Cutanda Henrquez F. Comparison of IPSM 1990 photon dosimetry code of practice with IAEA TRS-398 and AAPM TG-51. *J Appl Clin Med Phys*. 2009;10(1):2810.
26. Andreo P, Burns DT, Hohlfeld K, Bundesanstalt, et al. *An international code of practice for dosimetry based on standards of absorbed dose to water*; 2006.
27. Akbas U, Donmez Kesen N, Koksal C, Bilge H. Surface and buildup region dose measurements with Markus parallel-plate ionization chamber, GafChromic EBT3 film, and MOSFET detector for high-energy photon beams. *Adv. High Energy Phys*. 2016;2016:1–10.
28. Ashokkumar S, Ganesh KM, Ramalingam K, Karthikeyan K, Jagadheeskumar N. Dosimetric validation of volumetric modulated arc therapy with three 6MV beam-matched linear accelerators. *Asian Pac J Cancer Prev*. 2017;18(12):3439–3444.
29. Beyer GP. Commissioning measurements for photon beam data on three TrueBeam linear accelerators, and comparison with Trilogy and Clinac 2100 linear accelerators. *J Appl Clin Med Phys*. 2013;14:273–288.